

Searching for light long-lived particles at SHiNESS

Zeren Simon Wang^{a,b} Yu Zhang^{c,1} Wei Liu^{d,2}

^a*Department of Physics, National Tsing Hua University, Hsinchu 300, Taiwan*

^b*Center for Theory and Computation, National Tsing Hua University, Hsinchu 300, Taiwan*

^c*School of Physics, Hefei University of Technology, Hefei 230601, China*

^d*Department of Applied Physics and MIIT Key Laboratory of Semiconductor Microstructure and Quantum Sensing, Nanjing University of Science and Technology, Nanjing 210094, China*

E-mail: wzs@mx.nthu.edu.tw, dayu@hfut.edu.cn, wei.liu@njust.edu.cn

ABSTRACT: Recently Soleti et al. [*JHEP03(2024)148*] proposed a new experiment called SHiNESS at the upcoming European Spallation Source (ESS) facility, making use of the 2-GeV proton beam there impinging on a fixed target, in order to search for hidden sterile neutrinos that could lie in different mass ranges and arise with distinct signatures. Such signatures include excesses in electron-positron pairs that may originate from displaced decays of long-lived particles (LLPs). At the ESS, the dominant sources of such LLPs are decays at rest of π^+ mesons and μ^+ leptons. We choose to investigate theoretical scenarios of long-lived light binos in the R-parity-violating supersymmetry and long-lived weak-violating electrophilic axionlike particles, as these LLPs can be produced from decays of π^+ and μ^+ . Since the π^+ 's and μ^+ 's decay at rest at the ESS, we compute the spectra of the therefrom produced LLPs, and thus estimate the expected sensitivity reach of SHiNESS to the LLPs in these two scenarios. Our calculation shows that in most of the relevant benchmark scenarios, SHiNESS can probe large parameter regions of these models beyond the existing bounds, in just a couple of years of data-collection time.

¹Corresponding author.

²Corresponding author.

Contents

1	Introduction	1
2	Theoretical models	3
2.1	Light binos in the RPV-SUSY	3
2.2	Electrophilic ALPs with weak-violating couplings	5
3	Experimental setup	7
4	Numerical results	10
4.1	Light binos	10
4.2	Weak-violating ALPs coupled to electrons	15
5	Conclusions	15
A	Computation procedure of N_S^{90}	17

1 Introduction

The upcoming European Spallation Source (ESS) [1] facility is currently under construction on the outskirts of Lund, Sweden, and is expected to start operation in 2025. With protons impinging on a fixed target, a large flux of neutrons are produced. Meanwhile, a large number of light mesons including charged pions also arise, serving as the most intense source of neutrinos in the world. This allows to probe various forms of new physics in the neutrino sector. For instance, the future ESS Neutrino Super Beam (ESS ν SB) [2] can be utilized for searches for light sterile neutrinos [3–5]. To leverage this unique opportunity for searching for light new physics at the ESS, in Ref. [6] a new experiment called Search for Hidden Neutrinos at the ESS (SHiNESS) has been proposed, consisting of an active volume of 42 tons of liquid scintillator to be placed 25 meters away from the beam target. Besides determining whether an eV-scale sterile neutrino can explain the short-baseline neutrino anomalies observed at various neutrino experiments in the past, and more precisely measuring the unitarity of active-neutrino mixing matrix, the SHiNESS experiment can search for long-lived MeV-scale heavy neutral leptons (HNLs) that mix with active neutrinos, and is projected to place new bounds with only 2 years of data acquisition.

In this work, we explore the capability of the SHiNESS experiment to probe long-lived particles (LLPs)¹ in additional theoretical scenarios of feebly interacting particles. Indeed, in recent years after the observation of the Higgs boson at the LHC, lack of discovery of heavy fundamental particles that decay promptly as often predicted by new physics (NP)

¹See Refs. [7–10] for recent reviews on LLP models and searches.

beyond the Standard Model (BSM) has led to increasingly stronger lower bounds on their masses and shifted more attention towards non-traditional forms of NP signatures. These include displaced objects that are often associated with light LLPs. For example, at the LHC, a list of “far detectors” have been proposed, dedicated to LLP searches, such as FASER [11–13], CODEX-b [14, 15], and MATHUSLA [9, 16, 17]; in particular, FASER has been initiated since the start of Run 3 and published its early results [18, 19]. These experiments have been shown to be particularly promising in searching for light LLPs in the MeV-GeV mass range predicted in a large class of BSM theories. Here, we focus on the proposed SHiNESS experiment, where π^+ mesons are produced in large numbers and decay at rest. We consequently study the experiment’s potential in searching for light LLPs produced in decays of π^+ mesons and μ^+ leptons which also originate from π^+ decays.

Concretely, we consider light binos in the R-parity-violating supersymmetry (RPV-SUSY) [20–22], and weak-violating electrophilic axionlike particles (ALPs) [23], as benchmark models. In the RPV-SUSY, the lightest neutralino with a GeV-scale mass [24], which is necessarily bino-like [25, 26], is still allowed by all astrophysical and cosmological bounds [27–33] if we lift the GUT relation between the gauginos, $M_1 \approx 0.5 M_2$ [34, 35], the light bino is unstable to avoid overclosing the Universe [36], and the dark matter does not consist of the lightest neutralino [37–42]. The lightest neutralino should also be the lightest supersymmetric particle. The light bino can decay via RPV couplings, and if its mass is small, it has a long lifetime. Recent phenomenological studies on long-lived light binos in the RPV-SUSY can be found in, e.g. Refs. [43–49].

ALPs could solve the strong CP problem [50–52] and in addition, serve as a dark-matter candidate [53–59], among other motivations. ALPs are often conceived as arising from the breaking of a global U(1) Peccei-Quinn (PQ) [60] symmetry as pseudo-Nambu-Goldstone bosons. They are predicted to be long-lived for their feeble couplings with SM particles, even with masses in the MeV-GeV range. In this work, we focus on electrophilic ALPs with weak-violating couplings [23]. In this case, a four-point vertex arises between an ALP, a W -boson, an electron, and an electron neutrino, with no helicity suppression present. Some recent phenomenological works covering long-lived ALPs include Refs. [61–67].

We emphasize that for the installation of the SHiNESS experiment, no upgrade to the beamline is required, and the experiment can start taking data as soon as the ESS launches its operation. Moreover, as we will show, strong limits beyond current bounds on the considered models can be obtained in just a few years, strongly motivating the implementation of SHiNESS.

This paper is structured as follows. In Sec. 2 we introduce the theoretical models we study, and in Sec. 3 we detail the setup of the SHiNESS experiment. Sec. 4 is devoted to presenting numerical results of the projected sensitivity reach of SHiNESS. At the end, we conclude the work in Sec. 5 with a summary of our findings.

2 Theoretical models

2.1 Light binos in the RPV-SUSY

In the RPV-SUSY, we have the following superpotential containing lepton-number-violating (LNV) and baryon-number-violating (BNV) terms, in addition to the usual R-parity-conserving terms:

$$W_{\text{RPV}} = \kappa_i L_i H_u + \frac{1}{2} \lambda_{ijk} L_i L_j \bar{E}_k + \lambda'_{ijk} L_i Q_j \bar{D}_k + \frac{1}{2} \lambda''_{ijk} \bar{U}_i \bar{D}_j \bar{D}_k, \quad (2.1)$$

where the operators in the first and the second lines do not conserve the lepton number and the baryon number, respectively, and $i, j, k = 1, 2, 3$ are generation indices. κ_i are couplings of mass dimension 1, and λ , λ' , and λ'' are dimensionless couplings. Here, the factor $\frac{1}{2}$ is attached to the operators $LL\bar{E}$ and $\bar{U}\bar{D}\bar{D}$ because these operators possess the anti-symmetry property such that $\lambda_{ijk} = -\lambda_{jik}$ and $\lambda''_{ijk} = -\lambda''_{ikj}$. In this work, we assume that only λ and λ' couplings with certain flavor combinations are non-zero; this can be theoretically realized, as the bilinear term can be rotated away at a given energy scale [68, 69] and the BNV term can be vanishing if, for example, the baryon-triality symmetry is imposed [70–76].

As discussed in Sec. 1, a light MeV-scale bino is allowed and can be long-lived for tiny RPV couplings. For the SHiNESS experiment, we focus on LLPs produced in π^+ and μ^+ decays and on the final-state signature of an electron-positron pair from the $\tilde{\chi}_1^0$ decays. The π^+ decays into a light bino can be induced by the λ'_{111} or λ'_{211} couplings, while the signal decays of the μ^+ lepton and the bino can be mediated by various λ couplings. In Table 1 we summarize the possible RPV benchmark scenarios to study. In each benchmark scenario, we assume only two RPV LNV couplings are non-vanishing, mediating production and decay of the lightest neutralino, respectively, except in one benchmark **B3.1** where only a single coupling λ_{121} is assumed to be non-zero and it leads to both the production and decay of the light bino. Moreover, in certain benchmarks the decay coupling can also induce kinematically allowed production mode of the binos; these contributions are taken into account. Specifically, in Table 1, we list the production and decay couplings for the light bino, as well as the corresponding signal processes. We note that in benchmark scenarios **B1.1** and **B2.1**, λ_{121} are taken as the decay coupling. However, in principle, it also induces bino production from μ^+ -lepton decay, $\mu^+ \rightarrow \tilde{\chi}_1^0 \bar{\nu}_e e^+$; this production mode is not included in our computation because in these benchmarks we focus on bino production in π^+ decays. On the other hand, in benchmark scenarios **B4.1**, **B5.1**, and **B6.1**, since we are considering binos produced from μ^+ -lepton decays, we include the contributions of the decay coupling λ_{121} to the bino production from μ^+ decays. In addition, for kinematical reasons, the production couplings in general induce no decays of the light bino in the interested mass range of the listed benchmark scenarios. One exception is in **B1.1** and **B1.2**, where the decay $\tilde{\chi}_1^0 \rightarrow \pi^0 \nu_e^{(-)}$ can, in principle, take place via λ'_{111} , but the allowed bino mass window, $m_{\pi^0} < m_{\tilde{\chi}_1^0} < m_{\pi^+}$, is tiny, and therefore we ignore this case. Also,

Benchmark	λ_P	Prod. via λ_P	λ_D	Decay via λ_D	Prod. via λ_D	Decay via λ_P
B1.1	λ'_{111}	$\pi^+ \rightarrow e^+ \tilde{\chi}_1^0$	λ_{121}	$\tilde{\chi}_1^0 \rightarrow \begin{smallmatrix} (-) \\ \nu \end{smallmatrix} \mu e^+ e^-$	$\mu^+ \rightarrow \tilde{\chi}_1^0 \bar{\nu}_e e^+$	—
B1.2			λ_{131}	$\tilde{\chi}_1^0 \rightarrow \begin{smallmatrix} (-) \\ \nu \end{smallmatrix} \tau e^+ e^-$	—	—
B2.1	λ'_{211}	$\pi^+ \rightarrow \mu^+ \tilde{\chi}_1^0$	λ_{121}	$\tilde{\chi}_1^0 \rightarrow \begin{smallmatrix} (-) \\ \nu \end{smallmatrix} \mu e^+ e^-$	$\mu^+ \rightarrow \tilde{\chi}_1^0 \bar{\nu}_e e^+$	—
B2.2			λ_{131}	$\tilde{\chi}_1^0 \rightarrow \begin{smallmatrix} (-) \\ \nu \end{smallmatrix} \tau e^+ e^-$	—	—
B3.1	λ_{121}	$\mu^+ \rightarrow \tilde{\chi}_1^0 \bar{\nu}_e e^+$	λ_{121}	$\tilde{\chi}_1^0 \rightarrow \begin{smallmatrix} (-) \\ \nu \end{smallmatrix} \mu e^+ e^-$	Redundant	Redundant
B3.2			λ_{131}	$\tilde{\chi}_1^0 \rightarrow \begin{smallmatrix} (-) \\ \nu \end{smallmatrix} \tau e^+ e^-$	—	$\tilde{\chi}_1^0 \rightarrow \begin{smallmatrix} (-) \\ \nu \end{smallmatrix} \mu e^+ e^-$
B4.1	λ_{122}	$\mu^+ \rightarrow \tilde{\chi}_1^0 \nu_\mu e^+$	λ_{121}	$\tilde{\chi}_1^0 \rightarrow \begin{smallmatrix} (-) \\ \nu \end{smallmatrix} \mu e^+ e^-$	$\mu^+ \rightarrow \tilde{\chi}_1^0 \bar{\nu}_e e^+$	—
B4.2			λ_{131}	$\tilde{\chi}_1^0 \rightarrow \begin{smallmatrix} (-) \\ \nu \end{smallmatrix} \tau e^+ e^-$	—	—
B5.1	λ_{321}	$\mu^+ \rightarrow \tilde{\chi}_1^0 \bar{\nu}_\tau e^+$	λ_{121}	$\tilde{\chi}_1^0 \rightarrow \begin{smallmatrix} (-) \\ \nu \end{smallmatrix} \mu e^+ e^-$	$\mu^+ \rightarrow \tilde{\chi}_1^0 \bar{\nu}_e e^+$	—
B5.2			λ_{131}	$\tilde{\chi}_1^0 \rightarrow \begin{smallmatrix} (-) \\ \nu \end{smallmatrix} \tau e^+ e^-$	—	—
B6.1	λ_{312}	$\mu^+ \rightarrow \tilde{\chi}_1^0 \nu_\tau e^+$	λ_{121}	$\tilde{\chi}_1^0 \rightarrow \begin{smallmatrix} (-) \\ \nu \end{smallmatrix} \mu e^+ e^-$	$\mu^+ \rightarrow \tilde{\chi}_1^0 \bar{\nu}_e e^+$	—
B6.2			λ_{131}	$\tilde{\chi}_1^0 \rightarrow \begin{smallmatrix} (-) \\ \nu \end{smallmatrix} \tau e^+ e^-$	—	—

Table 1. Summary of the benchmark scenarios of the light binos in the RPV-SUSY. For benchmarks **B3.1**-**B6.2**, the μ^+ leptons are produced in $\pi^+ \rightarrow \mu^+ \nu_\mu$ decays at rest at the ESS. The lightest neutralino is of Majorana nature and can hence decay to both charge-conjugated channels. “—” means either theoretically irrelevant, or kinematically forbidden.

in **B3.1** by definition the production and decay couplings are identical. Finally, in **B3.2**, the production coupling λ_{121} can induce the $\tilde{\chi}_1^0 \rightarrow \begin{smallmatrix} (-) \\ \nu \end{smallmatrix} \mu e^+ e^-$ decays which are taken into account in the numerical computation.

To compute the production rates of the light bino from pion and muon decays via λ' and λ couplings, respectively, we resort to the analytic expressions provided in Refs. [43, 77], while the decay widths’ computation of the light bino via λ couplings follows the computation procedure given in Ref. [77].

We now discuss the present bounds on the relevant RPV couplings. These bounds stem from either measurements on low-energy observables [78] or recast of past searches for long-lived HNLs [77].

For the coupling λ'_{111} , both measurements of neutrinoless double-beta ($0\nu\beta\beta$) decays and existing bounds on long-lived HNLs provide the leading limits on $\lambda'_{111}/m_{\tilde{\chi}_1^0}^2$ as functions of the lightest neutralino’s mass $m_{\tilde{\chi}_1^0}$. The bound from $0\nu\beta\beta$ decays on the coupling is expressed as follows [79–82],

$$\lambda'_{111} < 5.2 \cdot 10^{-4} \cdot \left(\frac{m_{\tilde{e}}}{100 \text{ GeV}} \right)^2 \cdot \sqrt{\frac{m_{\tilde{\chi}_1^0}}{100 \text{ GeV}}}, \quad (2.2)$$

where $m_{\tilde{e}}$ is the selectron’s mass. The reinterpretation of the HNL searches’ results in terms of the light binos in the RPV-SUSY was performed in Ref. [77], and its Fig. 2 shows that these bounds are stronger than those from the $0\nu\beta\beta$ decays for $m_{\tilde{\chi}_1^0}$ roughly between 30 MeV and 130 MeV.

Similarly, bounds on λ'_{211} have been obtained from both measurements on $R_\pi = \Gamma(\pi \rightarrow e\nu)/\Gamma(\pi \rightarrow \mu\nu)$ [83] and recast of HNL searches [77]. The former gives a bound of

$$\lambda'_{211} < 0.059 \times \frac{m_{\tilde{d}_R}}{100 \text{ GeV}}, \quad (2.3)$$

where $m_{\tilde{d}_R}$ labels the mass of a right-handed sdown quark. However, Fig. 2 of Ref. [77] shows that reinterpretation of the HNL searches leads to the strongest bounds on $\lambda'_{211}/m_{\tilde{f}}^2$ for the light bino's mass below approximately 33 MeV.

The involved λ couplings all receive bounds from low-energy processes, as listed in Ref. [78], and we reproduce them here:

$$\lambda_{121} < 0.049 \cdot \frac{m_{\tilde{e}_R}}{100 \text{ GeV}}, \lambda_{122} < 0.049 \cdot \frac{m_{\tilde{\mu}_R}}{100 \text{ GeV}}, \quad (2.4)$$

$$\lambda_{131} < 0.062 \cdot \frac{m_{\tilde{e}_R}}{100 \text{ GeV}}, \quad (2.5)$$

$$\lambda_{321} < 0.070 \cdot \frac{m_{\tilde{e}_R}}{100 \text{ GeV}}, \lambda_{312} < 0.062 \cdot \frac{m_{\tilde{\mu}_R}}{100 \text{ GeV}}. \quad (2.6)$$

Here, \tilde{e}_R and $\tilde{\mu}_R$ denote right-handed selectron and smuon, respectively. Among these constraints, the bounds on λ_{121} and λ_{122} originate from charged-current universality [83]. The upper limits on λ_{131} were derived from measurements of $R_\tau = \Gamma(\tau \rightarrow e\nu\bar{\nu})/\Gamma(\tau \rightarrow \mu\nu\bar{\nu})$ [83]. Moreover, current bounds on λ_{321} and λ_{312} stem from measurements on $R_{\tau\mu} = \Gamma(\tau \rightarrow \mu\nu\bar{\nu})/\Gamma(\mu \rightarrow e\nu\bar{\nu})$ [84].

In addition, the λ_{121} , λ_{122} , and λ_{321} couplings are also bounded from uncertainty on the muon decay width of $\mu^\pm \rightarrow e^\pm + \text{invisible}$ [50] ($\sigma_{\Gamma(\mu^\pm \rightarrow e^\pm + \text{invis.})}$) as functions of the $m_{\tilde{\chi}_1^0}$, as given in Fig. 6 of Ref. [77]. The results are comparable with the bounds obtained from low-energy observables.

Besides the single-coupling bounds, there are strong constraints on the product of certain pairs of RPV couplings. Relevant for us are the bounds shown below:

$$\sqrt{\lambda_{121}\lambda_{122}} < 8.4 \times 10^{-4} \frac{m_{\tilde{\nu}_{\mu L}}}{100 \text{ GeV}}, \quad (2.7)$$

$$\sqrt{\lambda_{121}\lambda'_{111}} < 2.0 \times 10^{-4} \frac{m_{\tilde{\nu}_{e L}}}{100 \text{ GeV}}, \quad (2.8)$$

where the two bounds were derived from considerations of measurements on $\mu \rightarrow 3e$ [85] and on $\mu\text{Ti} \rightarrow e\text{Ti}$ [86, 87], respectively, and $m_{\tilde{\nu}_{\mu L}}$ and $m_{\tilde{\nu}_{e L}}$ are masses of left-handed muon sneutrino and electron sneutrino, respectively.

Finally, in this work, we assume degenerate sfermion masses $m_{\tilde{f}}$ for simplicity.

2.2 Electrophilic ALPs with weak-violating couplings

We consider an ALP, a , coupled to electrons only, and study the following signal processes: $\pi^+ \rightarrow e^+ \nu_e a$ and $a \rightarrow e^+ e^-$, where a can be long-lived for small couplings to the electrons. If the ALP is radiated off from the electron in the charged-pion decays, the process is strongly suppressed by helicity flip. However, as pointed out in Ref. [23], a four-point vertex between an ALP, a W -boson, a charged lepton, and a neutrino, should arise for ALPs with weak-violating couplings with charged leptons and was previously missed in

the literature. The four-point vertex can result in large rates of $\pi^+ \rightarrow e^+ \nu_e a$ with no helicity-flip suppression. Here, we focus on the following effective Lagrangian with a weak-violating term [23, 67],

$$\mathcal{L} \supset \partial_\mu a \frac{c_{ee}}{2\Lambda} \bar{e} \gamma^\mu \gamma_5 e, \quad (2.9)$$

which, after integration by part is applied, is transformed to the following terms,

$$\begin{aligned} \mathcal{L} \supset & i \frac{c_{ee} m_e}{\Lambda} a \bar{e} \gamma_5 e + \frac{ig}{2\sqrt{2}} \frac{c_{ee}}{\Lambda} a (\bar{e} \gamma^\mu P_L \nu_e) W_\mu^- \\ & + \dots + \text{h.c.}, \end{aligned} \quad (2.10)$$

where g is the SU(2) coupling constant, c_{ee} is a dimensionless coupling between the ALP and the electrons, and m_e is the electron mass. Λ is the effective cut-off scale of new physics and P_L is the left-chiral projector. The dots denote a set of terms arising from chiral anomaly and irrelevant to the phenomenology in our study, and are therefore ignored here.

Both terms in Eq. (2.10) mediate the $\pi^+ \rightarrow e^+ \nu_e a$ decay, and for the computation of its decay width, we refer to Ref. [23]. The decay width of the ALP into an electron-positron pair is calculated with the following expression [67, 88, 89]

$$\Gamma(a \rightarrow e^+ e^-) = \frac{c_{ee}^2}{8\pi\Lambda^2} m_e^2 m_a \sqrt{1 - \frac{4m_e^2}{m_a^2}}, \quad (2.11)$$

where m_a is the ALP mass. Following the practice taken in Ref. [23], we assume that the ALP decays with a 100% branching ratio into an electron-positron pair, and ignore the loop-induced photon-pair decay mode (which is sub-dominant for the relevant mass range anyway).

The existing bounds on c_{ee}/Λ in the weak-violating scenario are obtained from various laboratory and astrophysical searches and observations [90–103]. In addition, rough potential projections of sensitivities, expected at the PIONEER experiment [104], kaon factories [105], as well as the LHC, are also available and reproduced from Ref. [23]. In particular, the latter corresponds to a benchmark value of 10^{-5} for the ratio $\text{Br}_W = \text{Br}(W^+ \rightarrow l^+ \nu_l a)/\text{Br}(W^+ \rightarrow e^+ \nu)$, expected at the future LHC.

At the end, we comment that Ref. [23] also studied a weak-preserving scenario where the contributions from the four-point vertex are vanishing. We explicitly checked and found that in this case the expected sensitivity reach of SHiNESS is already all excluded by the SLAC E137 experiment [93], if we restrict ourselves to the ALP coupled to electrons only, as the strong helicity suppression largely reduces the production rates of the ALP. If the ALP is coupled to muons only, it will be produced in $\pi^+ \rightarrow \mu^+ \nu_\mu a$ decays; in this case, the helicity suppression is negligible, but SHiNESS will still have no sensitivity, for kinematic reasons related to cut selections to be imposed on final-state leptons (see discussion in Sec. 3). Therefore, we do not include this weak-preserving scenario in the present study.

3 Experimental setup

At the upcoming ESS facility, a 2-GeV proton beam hits a rotating tungsten target, producing large numbers of neutrons, serving the facility's main purpose [1]. In total, 2.8×10^{23} protons on target are planned for each calendar year. In such proton-nucleus collisions, an enormous number of charged pions among other hadrons are produced. While negatively charged pions are absorbed by the nucleus before decaying, positively charged ones lose energy via ionization effects while they are traveling and finally decay at rest, leading to the following decay chain:

$$\pi^+ \rightarrow \mu^+ \nu_\mu, \quad \mu^+ \rightarrow e^+ \nu_e \bar{\nu}_\mu. \quad (3.1)$$

Simulation indicates a neutrino yield of 0.3 per flavor (ν_μ , ν_e , and $\bar{\nu}_\mu$) per proton, implying 8.5×10^{22} neutrinos per flavor per year produced from π^+ decays at rest [106]. Since the π^+ mesons decay to $\mu^+ \nu_\mu$ with a branching fraction of $\sim 99.99\%$ [50], this corresponds to 8.5×10^{22} π^+ mesons produced each year and decaying at rest. The μ^+ leptons produced from π^+ decays also undergo ionization processes and quickly decay at rest in the close vicinity [106, 107].

The SHiNESS experiment has been proposed to be installed at some available space inside the D03 experimental hall, with a distance of 25 meters away from the tungsten target. Further, the SHiNESS detector is supposed to be placed with a polar angle $\theta = 35^\circ$ in the backward direction of the incoming proton beam, for the purpose of background-event mitigation. The detector is planned to be a stainless-steel cylindrical tank of a 5.3-m height and a 3.3-m radius, containing an internal active volume of a 4-m height and a 2-m radius filled with loaded liquid scintillator. In this work, we treat the active volume inside as the fiducial volume of the detector.

The proposal of the SHiNESS detector focuses on the $e^- e^+$ -pair signature in the context of searches for LLPs such as long-lived HNLs. This aim is realized by installing arrays of photomultipliers. Further, with the ability to detect both Cherenkov photons and scintillation light, the SHiNESS detector has strong vertex resolution and can reconstruct particle directions. This is further enabled by distinguishing between the Cherenkov and scintillation light that is allowed by various strategies and hardware implementation such as photosensors for their excellent timing resolution. We refer to Ref. [6] for more detail. In this work, as already specified in the previous section, we also concentrate on the signature of excesses in the number of $e^- e^+$ events (coming from decays of long-lived binos or ALPs).

We follow Ref. [6] for a brief discussion on background estimates. The LLP search requires reconstruction of a vertex formed from two charged leptons. The two lepton signals should be separated in time within 100 ns, and both should have an energy larger than 17 MeV. In addition, the opening angle between the two leptons should be at least 15° . With these requirements, the main background sources are cosmic ray, charged-current ν_e interactions, neutral-current ν interactions, and $\bar{\nu}_e$ beam component. These sources sum up to about 61 background events per year. A large, 50% systematic uncertainty is assigned, corresponding to 31 events per year [6], and we take the same assumption in this work.

For this study, we take 2 years' operation time as a benchmark, and calculate the signal-event number for the exclusion bounds at 90% confidence level (C.L.) below. For two years' data-collection time, we have 122 ± 43.84 background events in total. Performing an unbinned χ^2 test at 90% C.L., we find the corresponding bound on NP signal-event number to be $N_S^{90} \approx 72.17$. For detail of this estimate, we refer to Appendix A.

We perform simulations in order to estimate the detector acceptance to the long-lived binos or ALPs, as well as the cut efficiencies on the energies and opening angle of the final-state electron and positron. Specifically, the kinematics of the final-state particles in two-body decays can be simply determined by the masses of the mother and daughter particles. For three-body decays, kinematically allowed, random values of transferred momentum squared are taken in order to compute the 4-momenta of the final-state particles. Additionally, the particles are boosted to the laboratory frame. These procedures allow to simulate the kinematics of the LLPs and their decay products including the final-state electron and positron. With the knowledge of these particles' kinematics, we proceed to compute the detector acceptance and cut efficiencies.

For each simulated event, we check first on the final-state electron and positron whether they pass the above-mentioned cuts. If the energy and opening-angle requirements are satisfied, the associated simulated LLP is taken for computing its decay probability inside the active volume of the SHiNESS detector. The probability of the i^{th} simulated LLP to pass the lepton cuts and to decay inside the fiducial volume of SHiNESS is calculated as follows

$$\epsilon_{i^{\text{th}} \text{ LLP}}^{\text{cut\&acc.}} = \begin{cases} 0, & \text{if failing the lepton cuts,} \\ \epsilon_{i^{\text{th}} \text{ LLP}}^{\text{f.v.}}, & \text{if passing these selections,} \end{cases} \quad (3.2)$$

where we include the cut requirements on the final-state electron and positron, and “f.v.” in $\epsilon_{i^{\text{th}} \text{ LLP}}^{\text{f.v.}}$ stands for “fiducial volume”, and “acc.” is abbreviation for “acceptance”. To compute $\epsilon_{i^{\text{th}} \text{ LLP}}^{\text{f.v.}}$, we assume that in the vertical dimension the target is located in the middle of the SHiNESS detector. In Fig. 1 we display a bird's-eye view of the experimental setup, where $\theta = 35^\circ$ and $D = 25$ m is the distance of the detector to the tungsten target. The center of SHiNESS is at $y = 0$. We consider only the positive- z hemisphere (requiring the z -component of the momentum $p_z > 0$ on the LLPs) and use the following formulas to

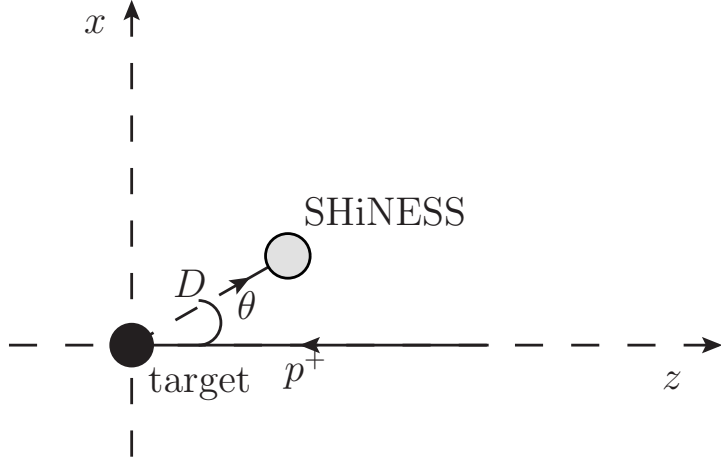


Figure 1. A bird's-eye view of the SHiNESS experiment. $\theta = 35^\circ$, and p^+ denotes the incoming 2-GeV proton beam. The distance of SHiNESS from the target is 25 meters. x and z label the axes.

compute $\epsilon_{i^{\text{th}}}^{\text{f.v.}}$ LLP,

$$\epsilon_{i^{\text{th}}}^{\text{f.v.}} \text{ LLP} = \sum_{j=1}^2 \delta\phi^j \cdot e^{-L_i^j/\lambda_i^z} \cdot \left(1 - e^{-\frac{L_i'^j}{\lambda_i^z}}\right), \quad (3.3)$$

$$L_i^j = \min\left(\max\left(d_h, \frac{d_v^j}{\tan\theta_i}\right), d_h + L_h\right), \quad (3.4)$$

$$L_i'^j = \min\left(\max\left(d_h, \frac{d_v^j + R}{\tan\theta_i}\right), d_h + L_h\right) - L_i^j, \quad (3.5)$$

$$\delta\phi^1 = 2 \cdot \arctan\left(\frac{L/2}{R/2 + d_v^1}\right)/(2\pi), \quad (3.6)$$

$$\delta\phi^2 = 2 \cdot \arctan\left(\frac{L/2}{R/2 + d_v^2}\right)/(2\pi), \quad (3.7)$$

$$d_v^1 = D \cdot \sin 35^\circ - R, \quad (3.8)$$

$$d_v^2 = D \cdot \sin 35^\circ, \quad (3.9)$$

where $L = 4$ m and $R = 2$ m are the height and radius of the fiducial volume, respectively. $d_h = D \cdot \cos 35^\circ$ is the longitudinal (along the z -axis) distance from the fixed target to the SHiNESS detector, and d_v^1 and d_v^2 are the distances along the x -axis from the target to the near end and middle position of SHiNESS, respectively. $\lambda_i^z = \beta_i^z \gamma_i c\tau$ is the boosted decay length of the i^{th} simulated LLP in the z -direction with β_i^z being the absolute speed, γ_i the boost factor, and $c\tau$ the proper decay length. $\delta\phi^j$ is the detector coverage in the azimuthal direction. The general idea of Eqs. (3.3) is to divide the detector into two parts (corresponding to $j = 1, 2$), one ($j = 2$) above the other ($j = 1$) along the x -axis, compute the LLP's decay probability inside each part, and sum them up in the end. While Eq. (3.3) is only an approximate formula, this approach of considering two parts reduces the error.

We note that despite the target wheel being 2.6-m wide [1], we have assumed above, for simplicity, that the target is point-like. Moreover, both π^+ mesons and μ^+ leptons are assumed to decay at rest at the interaction point on the target, considering the ionization effects as mentioned above. We expect this simplification of the setup to affect the final results to a rather minor extent (see discussion in Ref. [106]).

The signal-event number N_S is computed with the following formula,

$$N_S = N_{\text{LLP}} \cdot \epsilon_{\text{avg.}}^{\text{cut\&acc.}} \cdot \text{Br}(\text{LLP} \rightarrow e^- e^+ X), \quad (3.10)$$

where N_{LLP} is the total number of the LLPs expected to be produced in two years' operation of the ESS, $\text{Br}(\text{LLP} \rightarrow e^- e^+ X)$ is the decay branching ratio of the LLP into an electron-positron pair plus anything, and $\epsilon_{\text{avg.}}^{\text{cut\&acc.}}$ is evaluated with the following expression:

$$\epsilon_{\text{avg.}}^{\text{cut\&acc.}} = \frac{1}{N_{\text{sim.}}} \sum_{i=1}^{N_{\text{sim.}}} \epsilon_{i^{\text{th}} \text{ LLP}}^{\text{cut\&acc.}}. \quad (3.11)$$

Here, $N_{\text{sim.}}$ is the number of simulated signal events.

4 Numerical results

Following the discussion in the previous section, we present numerical results in this section, for the exclusion bounds at 90% C.L.

4.1 Light binos

For the theoretical model of long-lived light neutralinos in the RPV-SUSY, despite the multiple benchmark scenarios relevant in principle for LLP searches at SHiNESS as listed in Table 1, SHiNESS can probe large, unexcluded parameter space only in some of them.

For benchmarks **B1.1** and **B1.2**, strong bounds exist on the single coupling $\lambda'_{111}/m_{\tilde{f}}^2$ as functions of the light bino's mass, from $0\nu\beta\beta$ decays and HNL searches, cf. the discussion in Sec. 2. Additionally, for **B1.1**, the product bound given in Eq. (2.8) constrains the scenario tightly. Therefore, we choose to present only a sensitivity plot in Fig. 2 for **B1.2**, shown in the plane $\lambda'_{111}/m_{\tilde{f}}^2$ vs. $\lambda_{131}/m_{\tilde{f}}^2$, where we fix the light bino's mass at 20 MeV (black), 70 MeV (scarlet), and 120 MeV (green). The horizontal dashed curves are current upper bounds on $\lambda'_{111}/m_{\tilde{f}}^2$, where we have picked, for each bino-mass choice, the stronger limit between that derived from $0\nu\beta\beta$ decays and that from HNL searches. The vertical red curves are present upper limits on $\lambda_{131}/m_{\tilde{f}}^2$ for $m_{\tilde{f}} = 1$ TeV and 2 TeV (see Eq. (2.5)) which do not depend on $m_{\tilde{\chi}_1^0}$. We find that for all three choices of the bino mass, a triangle-shaped window that is still allowed in the shown parameter space can be excluded by SHiNESS in two years.

The benchmark scenarios **B2.1** and **B2.2** both assume a coupling λ'_{211} leading to the process $\pi^+ \rightarrow \mu^+ \tilde{\chi}_1^0$ producing the light bino. In this case, the light bino is produced with the maximally possible energy $m_{\pi^+} - m_{\mu^+} \approx 35$ MeV, since the π^+ 's decay at rest. As a result, it is impossible for the electron-positron pair produced in the decays of the light bino to pass the lepton-cut selections required in the search, and SHiNESS hence is

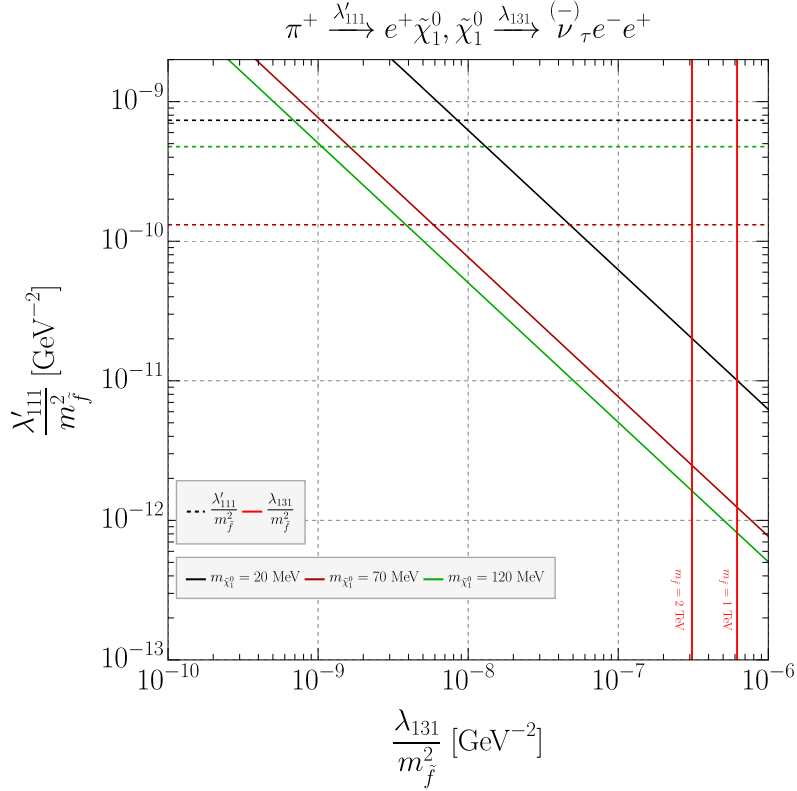


Figure 2. Sensitivity reach of SHiNESS in two years' data-collection time to the benchmark scenario **B1.2**, shown in the $(\lambda'_{131}/m_{\tilde{f}}^2, \lambda'_{111}/m_{\tilde{f}}^2)$ plane, for $m_{\tilde{\chi}_1^0} = 20$ MeV, 70 MeV, and 120 MeV. The horizontal dashed curves are present bounds on $\lambda'_{111}/m_{\tilde{f}}^2$ obtained from $0\nu\beta\beta$ decays [79–82] and recasting HNL searches [77], and the vertical dashed red curve are current limits on $\lambda'_{131}/m_{\tilde{f}}^2$ (see Eq. (2.5)).

insensitive to these benchmarks. Note that, of course, since in **B2.1** the coupling λ_{121} is present which can induce both $\mu^+ \rightarrow \tilde{\chi}_1^0 \bar{\nu}_e e^+$ and $\tilde{\chi}_1^0 \rightarrow \bar{\nu}_\mu e^+ e^-$ decays, SHiNESS should have sensitivities, but this decay chain reduces the scenario to **B3.1** and is hence not taken into account here.

The benchmark **B3.1** is interesting in that it is the only single-coupling scenario listed in Table 1, where the only non-vanishing coupling λ_{121} mediates both the production and decay of the lightest neutralino. We show a sensitivity plot in Fig. 3 in the $(m_{\tilde{\chi}_1^0}, \lambda_{121}/m_{\tilde{f}}^2)$ plane. Here, SHiNESS in two year's operation can probe $m_{\tilde{\chi}_1^0}$ up to right below the muon threshold. Compared to the existing bounds from charged-current universality (red horizontal curves), cf. Eq. (2.4), and those from the uncertainty on the measured decay width of $\mu^\pm \rightarrow e^\pm + \text{invisible}$ [77] (gray curve), we find that SHiNESS can exclude large parameter space for $m_{\tilde{\chi}_1^0}$ roughly between 20 MeV and 100 MeV, probing $\lambda_{121}/m_{\tilde{f}}^2$ down to as low as about 1.5×10^{-8} GeV $^{-2}$.

B3.2 is the only benchmark (besides **B3.1**) where the production coupling also induces kinematically-allowed bino decays. We choose to present the numerical results in Fig. 4,

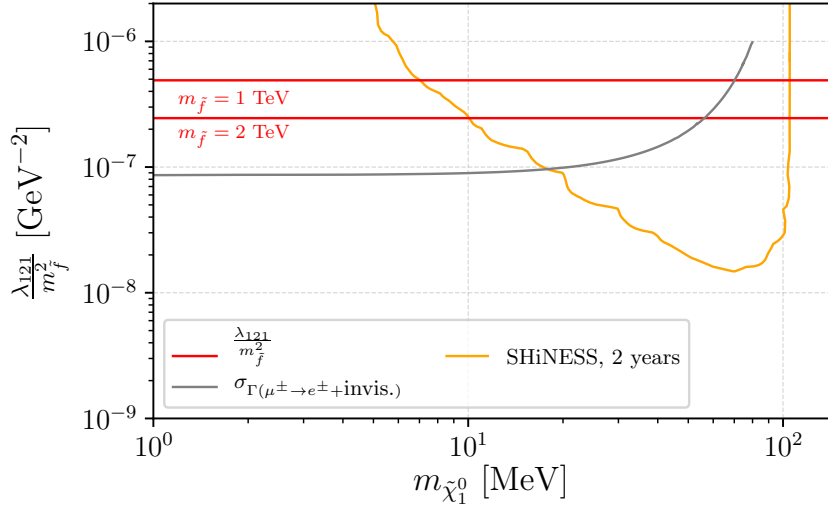


Figure 3. Sensitivity reach of SHiNESS to the benchmark **B3.1**, displayed in the plane $\lambda_{121}/m_{\tilde{f}}^2$ vs. $m_{\tilde{\chi}_1^0}$. The red dashed horizontal curves are current limits on $\lambda_{121}/m_{\tilde{f}}^2$, cf. Eq. (2.4), for $m_{\tilde{f}} = 1$ TeV and 2 TeV, and the gray dashed curve is the bound extracted from Ref. [77].

with two plots shown in the plane $\lambda_{121}/m_{\tilde{f}}^2$ vs. $\lambda_{131}/m_{\tilde{f}}^2$ and $\lambda_{121}/m_{\tilde{f}}^2 = \lambda_{131}/m_{\tilde{f}}^2$ vs. $m_{\tilde{\chi}_1^0}$, respectively. The present limits on both $\lambda_{121}/m_{\tilde{f}}^2$ (Eq. (2.4)) and $\lambda_{131}/m_{\tilde{f}}^2$ (Eq. (2.5)) are overlaid with blue and red curves, respectively, for both sfermion masses of 1 TeV and 2 TeV. Moreover, for $\lambda_{121}/m_{\tilde{f}}^2$, the bounds obtained by considering $\sigma_{\Gamma(\mu^\pm \rightarrow e^\pm + \text{invis.})}$ are also shown, in dashed lines with different colors corresponding to the chosen mass values (10 MeV, 20 MeV, and 60 MeV) of the light bino (upper panel) and in a gray solid line (lower panel). In the upper plot of Fig. 4, we observe that for small values of $\lambda_{131}/m_{\tilde{f}}^2$ the sensitivity curves become flat, reflecting the fact that the λ_{121} coupling alone can lead to sufficiently many signal events. We observe that for $m_{\tilde{\chi}_1^0} = 20$ MeV, 60 MeV, and 100 MeV, SHiNESS can probe large parameter space beyond the present bounds. Further, for increasing $m_{\tilde{\chi}_1^0}$ the sensitivity of SHiNESS is enhanced, except for the $m_{\tilde{\chi}_1^0} = 100$ MeV case where the phase-space suppression effect comes into play. The lower plot of Fig. 4, similar to Fig. 3, shows that SHiNESS can extend the current bounds largely in just two years, mainly for $m_{\tilde{\chi}_1^0}$ between about 20 MeV and 100 MeV.

For **B4.1**, the product bound as given in Eq. (2.7) is so strong that it has excluded all the parameter space that would be probed by SHiNESS if we set $\lambda_{121} = \lambda_{122}$. If the two non-vanishing λ couplings are independent, when $\lambda_{121}/m_{\tilde{f}}^2$ is sufficiently small, SHiNESS can only probe $\lambda_{122}/m_{\tilde{f}}^2$ values that are already excluded by the product bound. For larger values of $\lambda_{121}/m_{\tilde{f}}^2$, the search is insensitive to λ_{122} as the single coupling λ_{121} leading to both production and decay of the light bino alone would result in sufficiently many signal events (see Fig. 3). For these reasons, we do not present numerical results for **B4.1**.

The results of benchmarks **B5.1-B6.1** are all similar to those of the previous benchmarks, and we therefore refrain from showing them. We decide to present numerical results

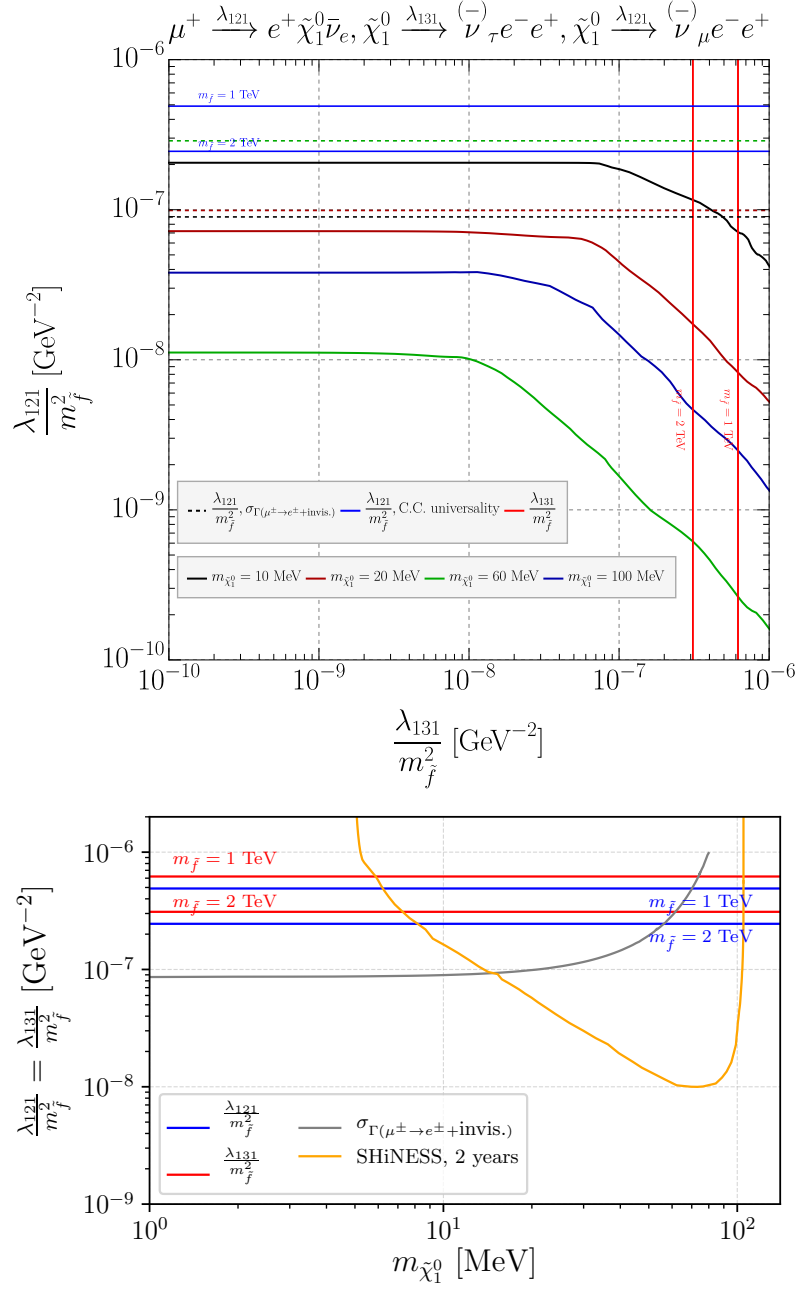


Figure 4. Sensitivity reach of SHiNESS to the benchmark **B3.2**. “C.C. universality” stands for “charged-current universality”, cf. Eq. (2.4).

for **B6.2**, where there is no available bound from reinterpretation of the HNL searches or $\sigma_{\Gamma(\mu^\pm \rightarrow e^\pm + \text{invis.})}$. We note that we choose not to show the results of **B4.2** because their conclusions are close to those of **B6.2**. In Fig. 5, we show two sensitivity plots in the plane λ_{312}/m_f^2 vs. λ_{131}/m_f^2 and $\lambda_{312}/m_f^2 = \lambda_{131}/m_f^2$ vs. $m_{\tilde{\chi}_1^0}$, respectively. In the upper plot, we fix the light neutralino’s mass at 10 MeV, 20 MeV, 60 MeV, and 100 MeV. The present

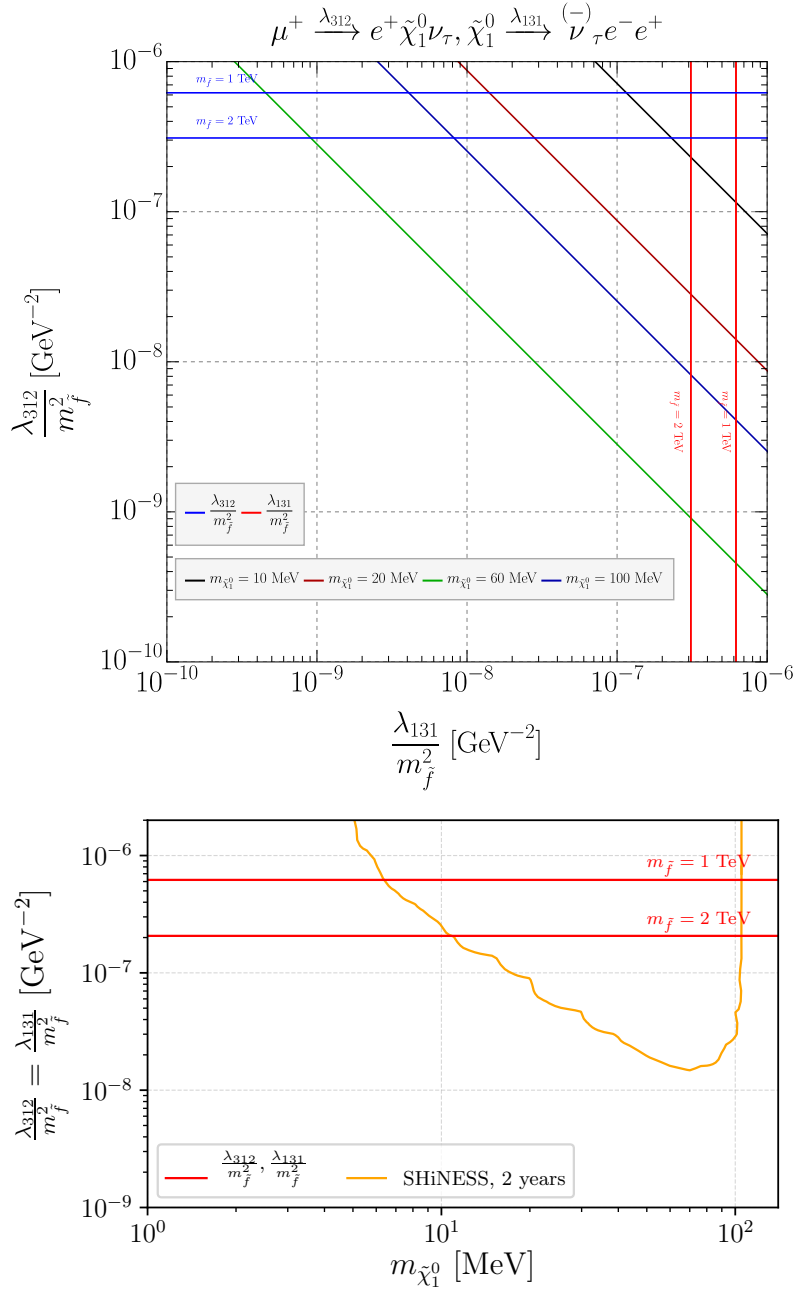


Figure 5. Sensitivity reach of SHiNESS to the benchmark **B6.2**, shown in the plane $\lambda_{312}/m_{\tilde{f}}^2$ vs. $\lambda_{131}/m_{\tilde{f}}^2$ (upper plot) and $\lambda_{312}/m_{\tilde{f}}^2 = \lambda_{131}/m_{\tilde{f}}^2$ vs. $m_{\tilde{\chi}_1^0}$ (lower plot).

bounds on the RPV couplings for $m_{\tilde{f}} = 1$ TeV and 2 TeV are shown, and we find that in the optimal case ($m_{\tilde{\chi}_1^0} = 60$ MeV), new parameter space up to more than two orders of magnitude beyond the current bounds can be excluded by SHiNESS in 2 years. The lower plot of Fig. 5 indicates that SHiNESS is predicted to probe unexcluded values of $\lambda_{312}/m_{\tilde{f}}^2 = \lambda_{131}/m_{\tilde{f}}^2$ more than one order of magnitude beyond the present limits in two

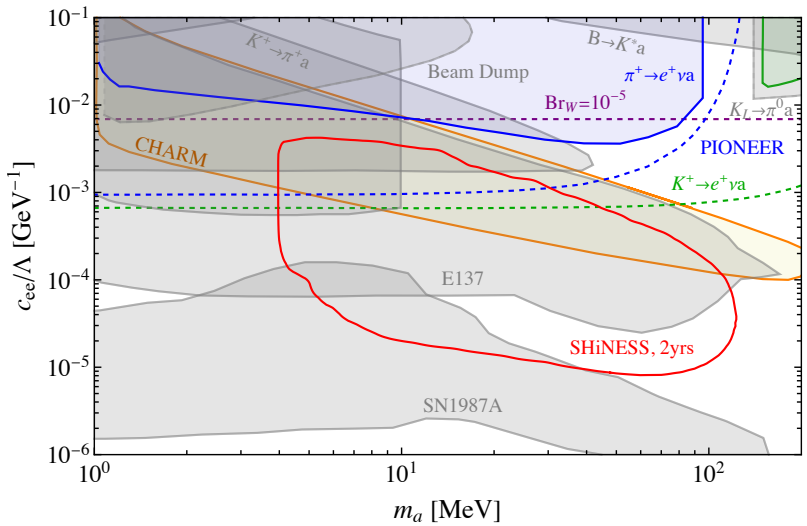


Figure 6. The projected sensitivity of SHiNESS with 2 years’ operation to the weak-violating electrophilic ALP, displayed in the $(m_a, c_{ee}/\Lambda)$ plane. The area inside the red curve can be excluded by SHiNESS. The gray area in the background, as well as the blue, green, and brown shaded regions, are the currently excluded parameter space, reproduced from Ref. [23]; see the text for detail. Ref. [23] also provided estimate of potential sensitivities from the PIONEER experiment [104] (dashed blue), kaon factories [105] (dashed green), as well as a benchmark of the LHC (dashed purple) [23]. See also the discussion in Sec. 2.2.

years, for $m_{\tilde{\chi}_1^0}$ between 10 MeV and 100 MeV.

4.2 Weak-violating ALPs coupled to electrons

The projected sensitivities of SHiNESS with 2-year data collation are presented in Fig. 6, in the plane c_{ee}/Λ vs. m_a . The current bounds stemming from electron beam-dump experiments [91–94], supernova SN1987A [97], and searches for flavor-changing-neutral-current decays of mesons [98–100], are shown in gray. Further, bounds obtained in searches for leptonic decays of charged mesons are displayed in blue for π^+ decays [101], in green for K^+ decays [102], and in brown for the CHARM experiment [103]. Particularly, rough estimates for potential bounds obtained from charged-pion and kaon decays are also overlaid with dashed lines, for the PIONEER experiment [104] (blue), kaon factories [105] (green), and the LHC (purple) [23]. We observe that while the potential of these future experiments is estimated to probe mainly the unexcluded parameter region of $c_{ee}/\Lambda \gtrsim 6 \times 10^{-4} \text{ GeV}^{-1}$, SHiNESS can be sensitive to a unique, allowed region $c_{ee}/\Lambda \sim \mathcal{O}(10^{-5}) \text{ GeV}^{-1}$ for m_a between roughly 10 MeV and 120 MeV.

5 Conclusions

In this work, we have investigated the potential of the SHiNESS experiment proposed to be installed at the ESS facility, to search for light long-lived particles. Following the SHiNESS proposal [6], we focus on the signature of LLPs at SHiNESS as excesses in electron-positron

pair events, and selection cuts on the final-state leptons are imposed in order to suppress background events to an acceptable level. Moreover, in order to estimate the cut efficiencies and acceptance of SHiNESS to LLPs, we have performed numerical simulations.

The focus of this work is on LLPs produced in rare decays at rest of π^+ mesons that arise from the 2-GeV proton beam at the facility hitting a rotating tungsten target and lose energy as they propagate. Specifically, we choose two theoretical models predicting light, MeV-scale LLPs, namely, a light bino in the RPV-SUSY, and a weak-violating electrophilic ALP. We consider production modes of the light bino including decays of $\pi^+ \rightarrow e^+ \tilde{\chi}_1^0$ and $\mu^+ \rightarrow e^+ \nu \tilde{\chi}_1^0$, where μ^+ stems from the $\pi^+ \rightarrow \mu^+ \nu_\mu$ decay at rest and also decays at rest immediately. The light bino then travels and decays inside SHiNESS into an electron-positron pair in association with a neutrino. Various benchmark scenarios, each with two non-vanishing RPV couplings mediating the production and decay of the light bino, respectively, are studied. Numerical results are then obtained and presented in the plane of either the production coupling vs. the decay coupling, or the RPV couplings (assumed to be equal) versus the light bino's mass. While for some benchmark scenarios we find SHiNESS is unable to probe unexcluded parameter space of the model for reasons of kinematics or too strong current bounds, for other benchmarks SHiNESS is predicted to be able to exclude large, new territories in the parameter space with just two years' data collection.

For the ALP, we focus on the $\pi^+ \rightarrow e^+ \nu_e a$ decay for its production and on $a \rightarrow e^- e^+$ for its signal decay. We assume a single, weak-violating term in an effective Lagrangian with the ALP coupled to a pair of electrons, that, after integration by parts, leads to both a helicity-suppressed three-point-vertex term, and a helicity-unsuppressed four-point-vertex term. The latter contribution, involving in the vertex an ALP, an electron, an electron neutrino, as well as a W -boson, results in large production rates of the ALP from the $\pi^+ \rightarrow e^+ \nu_e a$ decay. In the numerical results, we find that with solely two years' operation, SHiNESS can probe a unique, unexcluded part of the parameter space of $c_{ee}/\Lambda \sim \mathcal{O}(10^{-5})$ GeV^{-1} for m_a between 10 MeV and 120 MeV, complementary to other future experiments which would be sensitive to larger values of c_{ee}/Λ in a similar range of m_a .

Before closing, we note that in addition to decays of the π^+ mesons, decays of heavier pseudoscalar mesons such as K^+ can contribute to the LLP production. In spite of the smaller production rates, kaons may allow to probe heavier LLPs for kinematic reasons. We leave this possibility for future studies.

We conclude that with the ESS user program planned to begin in 2025, to implement a detector such as SHiNESS at the unallocated space in the D03 experimental hall is timely and has an exciting prospect for searching for BSM physics such as LLPs. We believe our work with the positive results highly motivates the construction and operation of the SHiNESS experiment.

Acknowledgements

We thank Liangwen Chen and Martin Schürmann for useful discussions. Y.Z. is supported by the National Natural Science Foundation of China under Grant No. 11805001 and the

Fundamental Research Funds for the Central Universities under Grant No. JZ2023HGTB0222. W.L. is supported by National Natural Science Foundation of China (Grant No. 12205153).

A Computation procedure of N_S^{90}

We explain the computation procedure of the number of NP signal events N_S required for estimating the sensitivity reach of the proposed SHiNESS experiment at 90% C.L., with an unbinned χ^2 test in a null hypothesis.

As mentioned in Sec. 3, the background-event number for the electron-positron pair search is expected to be 61 ± 31 per year after all event-selection requirements such as $E_{e^-}, E_{e^+} > 17$ MeV, are imposed [6]. We thus estimate that for two years SHiNESS should suffer from $N_B = 61 \times 2 = 122$ background events with an uncertainty of $\sigma_{N_B} = \sqrt{2} \times 31 \approx 43.84$ events. For the χ^2 distribution with one degree of freedom as is the case of this unbinned test, a critical value $\chi_{\text{c.v.}}^2$ of 2.71 is required for the 90% C.L.

To compute the χ^2 value we use the following expression,

$$\chi^2 = N_S^2 / \sigma_{N_B}^2, \quad (\text{A.1})$$

which is required to be larger than or equal to $\chi_{\text{c.v.}}^2$, in order to reject the null hypothesis, implying $N_S \geq \sqrt{\chi_{\text{c.v.}}^2} \cdot \sigma_{N_B} \approx 72.17$ corresponding to N_S^{90} .

References

- [1] R. Garoby et al., *The European Spallation Source Design*, *Phys. Scripta* **93** (2018), no. 1 014001.
- [2] A. Alekou et al., *The European Spallation Source neutrino super-beam conceptual design report*, *Eur. Phys. J. ST* **231** (2022), no. 21 3779–3955, [[arXiv:2206.01208](https://arxiv.org/abs/2206.01208)]. [Erratum: *Eur.Phys.J.ST* 232, 15–16 (2023)].
- [3] M. Blennow, P. Coloma, and E. Fernandez-Martinez, *Searching for sterile neutrinos at the ESSνSB*, *JHEP* **12** (2014) 120, [[arXiv:1407.1317](https://arxiv.org/abs/1407.1317)].
- [4] S. Kumar Agarwalla, S. S. Chatterjee, and A. Palazzo, *Physics potential of ESSνSB in the presence of a light sterile neutrino*, *JHEP* **12** (2019) 174, [[arXiv:1909.13746](https://arxiv.org/abs/1909.13746)].
- [5] M. Ghosh, T. Ohlsson, and S. Rosauro-Alcaraz, *Sensitivity to light sterile neutrinos at ESSnuSB*, *JHEP* **03** (2020) 026, [[arXiv:1912.10010](https://arxiv.org/abs/1912.10010)].
- [6] **SHiNESS** Collaboration, S. R. Soleti, P. Coloma, J. J. Gómez Cadenas, and A. Cabrera, *Search for hidden neutrinos at the European Spallation Source: the SHiNESS experiment*, *JHEP* **03** (2024) 148, [[arXiv:2311.18509](https://arxiv.org/abs/2311.18509)].
- [7] J. Alimena et al., *Searching for long-lived particles beyond the Standard Model at the Large Hadron Collider*, *J. Phys. G* **47** (2020), no. 9 090501, [[arXiv:1903.04497](https://arxiv.org/abs/1903.04497)].
- [8] L. Lee, C. Ohm, A. Soffer, and T.-T. Yu, *Collider Searches for Long-Lived Particles Beyond the Standard Model*, *Prog. Part. Nucl. Phys.* **106** (2019) 210–255, [[arXiv:1810.12602](https://arxiv.org/abs/1810.12602)]. [Erratum: *Prog.Part.Nucl.Phys.* 122, 103912 (2022)].
- [9] D. Curtin et al., *Long-Lived Particles at the Energy Frontier: The MATHUSLA Physics Case*, *Rept. Prog. Phys.* **82** (2019), no. 11 116201, [[arXiv:1806.07396](https://arxiv.org/abs/1806.07396)].

[10] J. Beacham et al., *Physics Beyond Colliders at CERN: Beyond the Standard Model Working Group Report*, *J. Phys. G* **47** (2020), no. 1 010501, [[arXiv:1901.09966](https://arxiv.org/abs/1901.09966)].

[11] J. L. Feng, I. Galon, F. Kling, and S. Trojanowski, *ForwArd Search ExpeRiment at the LHC*, *Phys. Rev. D* **97** (2018), no. 3 035001, [[arXiv:1708.09389](https://arxiv.org/abs/1708.09389)].

[12] **FASER** Collaboration, A. Ariga et al., *FASER’s physics reach for long-lived particles*, *Phys. Rev. D* **99** (2019), no. 9 095011, [[arXiv:1811.12522](https://arxiv.org/abs/1811.12522)].

[13] J. L. Feng et al., *The Forward Physics Facility at the High-Luminosity LHC*, *J. Phys. G* **50** (2023), no. 3 030501, [[arXiv:2203.05090](https://arxiv.org/abs/2203.05090)].

[14] V. V. Gligorov, S. Knapen, M. Papucci, and D. J. Robinson, *Searching for Long-lived Particles: A Compact Detector for Exotics at LHCb*, *Phys. Rev. D* **97** (2018), no. 1 015023, [[arXiv:1708.09395](https://arxiv.org/abs/1708.09395)].

[15] G. Aielli et al., *Expression of interest for the CODEX-b detector*, *Eur. Phys. J. C* **80** (2020), no. 12 1177, [[arXiv:1911.00481](https://arxiv.org/abs/1911.00481)].

[16] J. P. Chou, D. Curtin, and H. J. Lubatti, *New Detectors to Explore the Lifetime Frontier*, *Phys. Lett. B* **767** (2017) 29–36, [[arXiv:1606.06298](https://arxiv.org/abs/1606.06298)].

[17] **MATHUSLA** Collaboration, C. Alpigiani et al., *An Update to the Letter of Intent for MATHUSLA: Search for Long-Lived Particles at the HL-LHC*, [arXiv:2009.01693](https://arxiv.org/abs/2009.01693).

[18] **FASER** Collaboration, H. Abreu et al., *First Direct Observation of Collider Neutrinos with FASER at the LHC*, *Phys. Rev. Lett.* **131** (2023), no. 3 031801, [[arXiv:2303.14185](https://arxiv.org/abs/2303.14185)].

[19] **FASER** Collaboration, H. Abreu et al., *Search for dark photons with the FASER detector at the LHC*, *Phys. Lett. B* **848** (2024) 138378, [[arXiv:2308.05587](https://arxiv.org/abs/2308.05587)].

[20] R. Barbier et al., *R-parity violating supersymmetry*, *Phys. Rept.* **420** (2005) 1–202, [[hep-ph/0406039](https://arxiv.org/abs/hep-ph/0406039)].

[21] H. K. Dreiner, *An Introduction to explicit R-parity violation*, *Adv. Ser. Direct. High Energy Phys.* **21** (2010) 565–583, [[hep-ph/9707435](https://arxiv.org/abs/hep-ph/9707435)].

[22] R. N. Mohapatra, *Supersymmetry and R-parity: an Overview*, *Phys. Scripta* **90** (2015) 088004, [[arXiv:1503.06478](https://arxiv.org/abs/1503.06478)].

[23] W. Altmannshofer, J. A. Dror, and S. Gori, *New Opportunities for Detecting Axion-Lepton Interactions*, *Phys. Rev. Lett.* **130** (2023), no. 24 241801, [[arXiv:2209.00665](https://arxiv.org/abs/2209.00665)].

[24] F. Domingo and H. K. Dreiner, *Decays of a bino-like particle in the low-mass regime*, *SciPost Phys.* **14** (2023), no. 5 134, [[arXiv:2205.08141](https://arxiv.org/abs/2205.08141)].

[25] I. Gogoladze, J. D. Lykken, C. Macesanu, and S. Nandi, *Implications of a Massless Neutralino for Neutrino Physics*, *Phys. Rev. D* **68** (2003) 073004, [[hep-ph/0211391](https://arxiv.org/abs/hep-ph/0211391)].

[26] H. K. Dreiner, S. Heinemeyer, O. Kittel, U. Langenfeld, A. M. Weber, and G. Weiglein, *Mass Bounds on a Very Light Neutralino*, *Eur. Phys. J. C* **62** (2009) 547–572, [[arXiv:0901.3485](https://arxiv.org/abs/0901.3485)].

[27] J. A. Grifols, E. Masso, and S. Peris, *Photinos From Gravitational Collapse*, *Phys. Lett. B* **220** (1989) 591–596.

[28] J. R. Ellis, K. A. Olive, S. Sarkar, and D. W. Sciama, *Low Mass Photinos and Supernova SN1987A*, *Phys. Lett. B* **215** (1988) 404–410.

[29] K. Lau, *Constraints on supersymmetry from SN1987A*, *Phys. Rev. D* **47** (1993) 1087–1092.

[30] H. K. Dreiner, C. Hanhart, U. Langenfeld, and D. R. Phillips, *Supernovae and light neutralinos: SN1987A bounds on supersymmetry revisited*, *Phys. Rev. D* **68** (2003) 055004, [[hep-ph/0304289](#)].

[31] H. K. Dreiner, J.-F. Fortin, J. Isern, and L. Ubaldi, *White Dwarfs constrain Dark Forces*, *Phys. Rev. D* **88** (2013) 043517, [[arXiv:1303.7232](#)].

[32] S. Profumo, *Hunting the lightest lightest neutralinos*, *Phys. Rev. D* **78** (2008) 023507, [[arXiv:0806.2150](#)].

[33] H. K. Dreiner, M. Hanussek, J. S. Kim, and S. Sarkar, *Gravitino cosmology with a very light neutralino*, *Phys. Rev. D* **85** (2012) 065027, [[arXiv:1111.5715](#)].

[34] D. Choudhury and S. Sarkar, *A Supersymmetric resolution of the KARMEN anomaly*, *Phys. Lett. B* **374** (1996) 87–92, [[hep-ph/9511357](#)].

[35] D. Choudhury, H. K. Dreiner, P. Richardson, and S. Sarkar, *A Supersymmetric solution to the KARMEN time anomaly*, *Phys. Rev. D* **61** (2000) 095009, [[hep-ph/9911365](#)].

[36] P. Bechtle et al., *Killing the cMSSM softly*, *Eur. Phys. J. C* **76** (2016), no. 2 96, [[arXiv:1508.05951](#)].

[37] G. Belanger, F. Boudjema, A. Pukhov, and S. Rosier-Lees, *A Lower limit on the neutralino mass in the MSSM with nonuniversal gaugino masses*, in *10th International Conference on Supersymmetry and Unification of Fundamental Interactions (SUSY02)*, pp. 919–924, 12, 2002. [hep-ph/0212227](#).

[38] D. Hooper and T. Plehn, *Supersymmetric dark matter: How light can the LSP be?*, *Phys. Lett. B* **562** (2003) 18–27, [[hep-ph/0212226](#)].

[39] A. Bottino, N. Fornengo, and S. Scopel, *Light relic neutralinos*, *Phys. Rev. D* **67** (2003) 063519, [[hep-ph/0212379](#)].

[40] G. Belanger, F. Boudjema, A. Cottrant, A. Pukhov, and S. Rosier-Lees, *Lower limit on the neutralino mass in the general MSSM*, *JHEP* **03** (2004) 012, [[hep-ph/0310037](#)].

[41] D. Albornoz Vasquez, G. Belanger, C. Boehm, A. Pukhov, and J. Silk, *Can neutralinos in the MSSM and NMSSM scenarios still be light?*, *Phys. Rev. D* **82** (2010) 115027, [[arXiv:1009.4380](#)].

[42] L. Calibbi, J. M. Lindert, T. Ota, and Y. Takanishi, *Cornering light Neutralino Dark Matter at the LHC*, *JHEP* **10** (2013) 132, [[arXiv:1307.4119](#)].

[43] J. de Vries, H. K. Dreiner, and D. Schmeier, *R-Parity Violation and Light Neutralinos at SHiP and the LHC*, *Phys. Rev. D* **94** (2016), no. 3 035006, [[arXiv:1511.07436](#)].

[44] G. Cottin, J. C. Helo, N. A. Neill, F. Hernández-Pinto, and Z. S. Wang, *Searching for light neutralinos with a displaced vertex at the LHC*, *JHEP* **10** (2022) 095, [[arXiv:2208.12818](#)]. [Erratum: *JHEP* 06, 069 (2024)].

[45] J. Gehrlein and S. Ipek, *Long-lived $b\bar{\nu}\nu$ at the LHC*, *JHEP* **05** (2021) 020, [[arXiv:2103.01251](#)].

[46] D. Dercks, J. De Vries, H. K. Dreiner, and Z. S. Wang, *R-parity Violation and Light Neutralinos at CODEX-b, FASER, and MATHUSLA*, *Phys. Rev. D* **99** (2019), no. 5 055039, [[arXiv:1810.03617](#)].

[47] H. K. Dreiner, J. Y. Günther, and Z. S. Wang, *R-parity violation and light neutralinos at ANUBIS and MAPP*, *Phys. Rev. D* **103** (2021), no. 7 075013, [[arXiv:2008.07539](#)].

[48] H. K. Dreiner, D. Köhler, S. Nangia, and Z. S. Wang, *Searching for a single photon from lightest neutralino decays in R-parity-violating supersymmetry at FASER*, *JHEP* **02** (2023) 120, [[arXiv:2207.05100](https://arxiv.org/abs/2207.05100)].

[49] J. Y. Günther, J. de Vries, H. K. Dreiner, Z. S. Wang, and G. Zhou, *Long-lived neutral fermions at the DUNE near detector*, *JHEP* **01** (2024) 108, [[arXiv:2310.12392](https://arxiv.org/abs/2310.12392)].

[50] **Particle Data Group** Collaboration, R. L. Workman et al., *Review of Particle Physics*, *PTEP* **2022** (2022) 083C01.

[51] R. D. Peccei and H. R. Quinn, *Constraints Imposed by CP Conservation in the Presence of Instantons*, *Phys. Rev. D* **16** (1977) 1791–1797.

[52] R. D. Peccei, *The Strong CP problem and axions*, *Lect. Notes Phys.* **741** (2008) 3–17, [[hep-ph/0607268](https://arxiv.org/abs/hep-ph/0607268)].

[53] M. Dine and W. Fischler, *The Not So Harmless Axion*, *Phys. Lett. B* **120** (1983) 137–141.

[54] L. F. Abbott and P. Sikivie, *A Cosmological Bound on the Invisible Axion*, *Phys. Lett. B* **120** (1983) 133–136.

[55] J. Preskill, M. B. Wise, and F. Wilczek, *Cosmology of the Invisible Axion*, *Phys. Lett. B* **120** (1983) 127–132.

[56] D. J. E. Marsh, *Axion Cosmology*, *Phys. Rept.* **643** (2016) 1–79, [[arXiv:1510.07633](https://arxiv.org/abs/1510.07633)].

[57] G. Lambiase and S. Mohanty, *Hydrogen spin oscillations in a background of axions and the 21-cm brightness temperature*, *Mon. Not. Roy. Astron. Soc.* **494** (2020), no. 4 5961–5966, [[arXiv:1804.05318](https://arxiv.org/abs/1804.05318)].

[58] A. Auriol, S. Davidson, and G. Raffelt, *Axion absorption and the spin temperature of primordial hydrogen*, *Phys. Rev. D* **99** (2019), no. 2 023013, [[arXiv:1808.09456](https://arxiv.org/abs/1808.09456)].

[59] N. Houston, C. Li, T. Li, Q. Yang, and X. Zhang, *Natural Explanation for 21 cm Absorption Signals via Axion-Induced Cooling*, *Phys. Rev. Lett.* **121** (2018), no. 11 111301, [[arXiv:1805.04426](https://arxiv.org/abs/1805.04426)].

[60] R. D. Peccei and H. R. Quinn, *CP Conservation in the Presence of Instantons*, *Phys. Rev. Lett.* **38** (1977) 1440–1443.

[61] E. Bertholet, S. Chakraborty, V. Loladze, T. Okui, A. Soffer, and K. Tobioka, *Heavy QCD axion at Belle II: Displaced and prompt signals*, *Phys. Rev. D* **105** (2022), no. 7 L071701, [[arXiv:2108.10331](https://arxiv.org/abs/2108.10331)].

[62] R. T. Co, S. Kumar, and Z. Liu, *Searches for heavy QCD axions via dimuon final states*, *JHEP* **02** (2023) 111, [[arXiv:2210.02462](https://arxiv.org/abs/2210.02462)].

[63] A. Carmona, F. Elahi, C. Scherb, and P. Schwaller, *The ALPs from the top: searching for long lived axion-like particles from exotic top decays*, *JHEP* **07** (2022) 122, [[arXiv:2202.09371](https://arxiv.org/abs/2202.09371)].

[64] K. Cheung, J.-L. Kuo, P.-Y. Tseng, and Z. S. Wang, *Atmospheric axionlike particles at Super-Kamiokande*, *Phys. Rev. D* **106** (2022), no. 9 095029, [[arXiv:2208.05111](https://arxiv.org/abs/2208.05111)].

[65] K. Cheung, A. Soffer, Z. S. Wang, and Y.-H. Wu, *Probing charged lepton flavor violation with axion-like particles at Belle II*, *JHEP* **11** (2021) 218, [[arXiv:2108.11094](https://arxiv.org/abs/2108.11094)].

[66] K. Cheung, F.-T. Chung, G. Cottin, and Z. S. Wang, *Quark flavor violation and axion-like particles from top-quark decays at the LHC*, *JHEP* **07** (2024) 209, [[arXiv:2404.06126](https://arxiv.org/abs/2404.06126)].

[67] C.-T. Lu, *Lighting electroweak-violating ALP-lepton interactions at $e+e-$ and ep colliders*, *Phys. Rev. D* **108** (2023), no. 11 115029, [[arXiv:2210.15648](#)].

[68] L. J. Hall and M. Suzuki, *Explicit R-Parity Breaking in Supersymmetric Models*, *Nucl. Phys. B* **231** (1984) 419–444.

[69] H. K. Dreiner and M. Thormeier, *Supersymmetric Froggatt-Nielsen models with baryon and lepton number violation*, *Phys. Rev. D* **69** (2004) 053002, [[hep-ph/0305270](#)].

[70] H. K. Dreiner, C. Luhn, and M. Thormeier, *What is the discrete gauge symmetry of the MSSM?*, *Phys. Rev. D* **73** (2006) 075007, [[hep-ph/0512163](#)].

[71] L. E. Ibanez and G. G. Ross, *Discrete gauge symmetry anomalies*, *Phys. Lett. B* **260** (1991) 291–295.

[72] S. P. Martin, *A Supersymmetry primer*, *Adv. Ser. Direct. High Energy Phys.* **18** (1998) 1–98, [[hep-ph/9709356](#)].

[73] Y. Grossman and H. E. Haber, *(S)neutrino properties in R-parity violating supersymmetry. 1. CP conserving phenomena*, *Phys. Rev. D* **59** (1999) 093008, [[hep-ph/9810536](#)].

[74] H. K. Dreiner, C. Luhn, H. Murayama, and M. Thormeier, *Baryon triality and neutrino masses from an anomalous flavor $U(1)$* , *Nucl. Phys. B* **774** (2007) 127–167, [[hep-ph/0610026](#)].

[75] H. K. Dreiner, J. Soo Kim, and M. Thormeier, *A Simple baryon triality model for neutrino masses*, [arXiv:0711.4315](#).

[76] M. A. Bernhardt, S. P. Das, H. K. Dreiner, and S. Grab, *Sneutrino as Lightest Supersymmetric Particle in B_3 mSUGRA Models and Signals at the LHC*, *Phys. Rev. D* **79** (2009) 035003, [[arXiv:0810.3423](#)].

[77] H. K. Dreiner, D. Köhler, S. Nangia, M. Schürmann, and Z. S. Wang, *Recasting bounds on long-lived heavy neutral leptons in terms of a light supersymmetric R-parity violating neutralino*, *JHEP* **08** (2023) 058, [[arXiv:2306.14700](#)].

[78] B. C. Allanach, A. Dedes, and H. K. Dreiner, *Bounds on R-parity violating couplings at the weak scale and at the GUT scale*, *Phys. Rev. D* **60** (1999) 075014, [[hep-ph/9906209](#)].

[79] R. N. Mohapatra, *New Contributions to Neutrinoless Double beta Decay in Supersymmetric Theories*, *Phys. Rev. D* **34** (1986) 3457–3461.

[80] M. Hirsch, H. V. Klapdor-Kleingrothaus, and S. G. Kovalenko, *New constraints on R-parity broken supersymmetry from neutrinoless double beta decay*, *Phys. Rev. Lett.* **75** (1995) 17–20.

[81] M. Hirsch, H. V. Klapdor-Kleingrothaus, and S. G. Kovalenko, *Supersymmetry and neutrinoless double beta decay*, *Phys. Rev. D* **53** (1996) 1329–1348, [[hep-ph/9502385](#)].

[82] K. S. Babu and R. N. Mohapatra, *New vector - scalar contributions to neutrinoless double beta decay and constraints on R-parity violation*, *Phys. Rev. Lett.* **75** (1995) 2276–2279, [[hep-ph/9506354](#)].

[83] V. D. Barger, G. F. Giudice, and T. Han, *Some New Aspects of Supersymmetry R-Parity Violating Interactions*, *Phys. Rev. D* **40** (1989) 2987.

[84] F. Ledroit and S. G., *Rapport GDR-Supersymétrie*. ISN, Grenoble, 1998.

[85] D. Choudhury and P. Roy, *New constraints on lepton nonconserving R-parity violating couplings*, *Phys. Lett. B* **378** (1996) 153–158, [[hep-ph/9603363](#)].

[86] J. E. Kim, P. Ko, and D.-G. Lee, *More on R-parity and lepton family number violating couplings from muon(ium) conversion, and tau and pi0 decays*, *Phys. Rev. D* **56** (1997) 100–106, [[hep-ph/9701381](#)].

[87] K. Huitu, J. Maalampi, M. Raidal, and A. Santamaria, *New constraints on R-parity violation from mu e conversion in nuclei*, *Phys. Lett. B* **430** (1998) 355–362, [[hep-ph/9712249](#)].

[88] M. Bauer, M. Neubert, and A. Thamm, *Collider Probes of Axion-Like Particles*, *JHEP* **12** (2017) 044, [[arXiv:1708.00443](#)].

[89] M. Bauer, M. Heiles, M. Neubert, and A. Thamm, *Axion-Like Particles at Future Colliders*, *Eur. Phys. J. C* **79** (2019), no. 1 74, [[arXiv:1808.10323](#)].

[90] **BaBar** Collaboration, J. P. Lees et al., *Search for a Dark Photon in e^+e^- Collisions at BaBar*, *Phys. Rev. Lett.* **113** (2014), no. 20 201801, [[arXiv:1406.2980](#)].

[91] A. Konaka et al., *Search for Neutral Particles in Electron Beam Dump Experiment*, *Phys. Rev. Lett.* **57** (1986) 659.

[92] E. M. Riordan et al., *A Search for Short Lived Axions in an Electron Beam Dump Experiment*, *Phys. Rev. Lett.* **59** (1987) 755.

[93] J. D. Bjorken, S. Ecklund, W. R. Nelson, A. Abashian, C. Church, B. Lu, L. W. Mo, T. A. Numamaker, and P. Rassmann, *Search for Neutral Metastable Penetrating Particles Produced in the SLAC Beam Dump*, *Phys. Rev. D* **38** (1988) 3375.

[94] A. Bross, M. Crisler, S. H. Pordes, J. Volk, S. Errede, and J. Wrbanek, *A Search for Shortlived Particles Produced in an Electron Beam Dump*, *Phys. Rev. Lett.* **67** (1991) 2942–2945.

[95] L. Morel, Z. Yao, P. Cladé, and S. Guellati-Khélifa, *Determination of the fine-structure constant with an accuracy of 81 parts per trillion*, *Nature* **588** (2020), no. 7836 61–65.

[96] R. H. Parker, C. Yu, W. Zhong, B. Estey, and H. Müller, *Measurement of the fine-structure constant as a test of the Standard Model*, *Science* **360** (2018) 191, [[arXiv:1812.04130](#)].

[97] G. Lucente and P. Carenza, *Supernova bound on axionlike particles coupled with electrons*, *Phys. Rev. D* **104** (2021), no. 10 103007, [[arXiv:2107.12393](#)].

[98] **KTeV** Collaboration, A. Alavi-Harati et al., *Search for the rare decay $K(L) \rightarrow \pi^0 e^+ e^-$* , *Phys. Rev. Lett.* **93** (2004) 021805, [[hep-ex/0309072](#)].

[99] **LHCb** Collaboration, R. Aaij et al., *Angular analysis of the $B^0 \rightarrow K^{*0} e^+ e^-$ decay in the low- q^2 region*, *JHEP* **04** (2015) 064, [[arXiv:1501.03038](#)].

[100] **NA62** Collaboration, E. Cortina Gil et al., *Search for a feebly interacting particle X in the decay $K^+ \rightarrow \pi^+ X$* , *JHEP* **03** (2021) 058, [[arXiv:2011.11329](#)].

[101] **SINDRUM** Collaboration, R. Eichler et al., *Limits for Shortlived Neutral Particles Emitted μ^+ or π^+ Decay*, *Phys. Lett. B* **175** (1986) 101.

[102] A. A. Pobladuev et al., *Experimental study of the radiative decays $K+ \rightarrow \mu+ \nu \mu+ \nu$ and $K+ \rightarrow e+ \nu e+ \nu$* , *Phys. Rev. Lett.* **89** (2002) 061803, [[hep-ex/0204006](#)].

[103] **CHARM** Collaboration, F. Bergsma et al., *Search for Axion Like Particle Production in 400-GeV Proton - Copper Interactions*, *Phys. Lett. B* **157** (1985) 458–462.

[104] **PIONEER** Collaboration, W. Altmannshofer et al., *PIONEER: Studies of Rare Pion Decays*, [arXiv:2203.01981](#).

- [105] E. Goudzovski et al., *New physics searches at kaon and hyperon factories*, *Rept. Prog. Phys.* **86** (2023), no. 1 016201, [[arXiv:2201.07805](https://arxiv.org/abs/2201.07805)].
- [106] D. Baxter et al., *Coherent Elastic Neutrino-Nucleus Scattering at the European Spallation Source*, *JHEP* **02** (2020) 123, [[arXiv:1911.00762](https://arxiv.org/abs/1911.00762)].
- [107] R. L. Burman and W. C. Louis, *Neutrino physics at meson factories and spallation neutron sources*, *J. Phys. G* **29** (2003) 2499–2512.